

## Wideband channels

### 3.1 Deterministic wideband model

The time-invariant channel impulse response can be written as (1.6)

$$\begin{aligned} h(\tau) &= \sum_{n=1}^N a_n e^{j\phi_n} e^{-j2\pi f_c \tau_n} \delta(\tau - \tau_n) \\ &= \sum_{n=1}^N a_n e^{j\varphi_n} \delta(\tau - \tau_n) \end{aligned} \quad (3.1)$$

where  $\varphi_n = \phi_n - 2\pi f_c \tau_n$ .

Or, equivalently, its Fourier transform, the time-invariant transfer function (1.10)

$$H(f) = \int_{-\infty}^{\infty} h(\tau) e^{-j2\pi f \tau} d\tau = \sum_{n=1}^N a_n e^{j\varphi_n} e^{-j2\pi f \tau_n} \quad (3.2)$$

#### 3.1.1 1-wave model

If the receiver only detects one MPC in the delay domain :

$$H(f) = a_1 e^{j\varphi_1} e^{-j2\pi f \tau_1} \quad (3.3)$$

whose amplitude does not depend on baseband frequency  $f$  : the transmitted signal is multiplied by the same channel gain across the whole frequency band (i.e. there is no distortion due to the channel). It is said to experience **flat fading**.

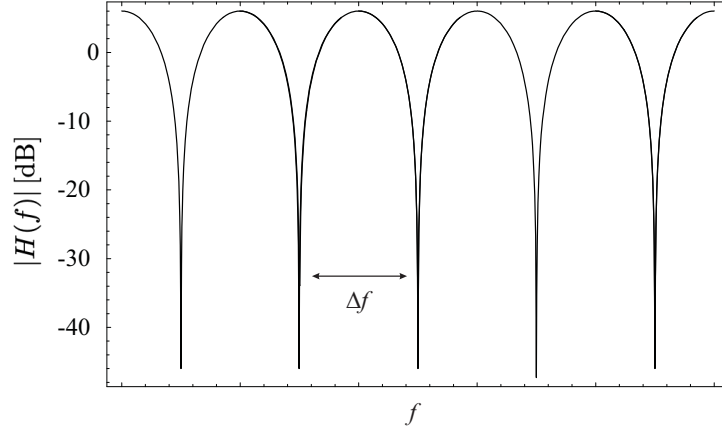


Figure 3.1 – 2-waves model : amplitude of the transfer function ( $a_1 = a_2 = 1$ , and  $\varphi_1 = \varphi_2 = 0$ )

### 3.1.2 2-waves model

If two MPC's are detected in the delay domain :

$$H(f) = a_1 e^{j\varphi_1} e^{-j2\pi f\tau_1} + a_2 e^{j\varphi_2} e^{-j2\pi f\tau_2} \quad (3.4)$$

whose amplitude is

$$\begin{aligned} |H(f)| &= \sqrt{(a_1 e^{j\varphi_1} e^{-j2\pi f\tau_1} + a_2 e^{j\varphi_2} e^{-j2\pi f\tau_2})(a_1 e^{-j\varphi_1} e^{j2\pi f\tau_1} + a_2 e^{-j\varphi_2} e^{j2\pi f\tau_2})} \\ &= \sqrt{a_1^2 + a_2^2 + 2a_1 a_2 \cos(\varphi_1 - \varphi_2) \cos(2\pi f \Delta\tau)} \end{aligned} \quad (3.5)$$

where  $\Delta\tau = \tau_2 - \tau_1$ .

Now, the amplitude of  $H$  depends on the frequency, and on the **difference** of propagation delays between the two MPC's. One example of (3.5) is drawn in dB scale in Figure 3.1. It can be seen that certain frequencies will be heavily damped by the channel so that the transmitted signal is distorted when detected by the receiver. The channel experiences **frequency selective fading**.

Frequency selectivity comes from the difference in propagation delays as shown by (3.5), i.e. from signal **time dispersion** during propagation. Eq (3.5) shows that the fre-

quency shift  $\Delta f$  between two fades of  $|H|$  is

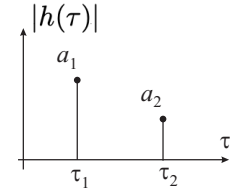
$$\Delta f = \frac{1}{\Delta \tau} \quad (3.6)$$

i.e. the larger the time dispersion  $\Delta \tau$ , the faster the frequency fading.

The channel **impulse response**  $h(\tau)$  (complex !) lists the detected MPC's in the delay domain. For instance in the 2-waves model :

$$h(\tau) = a_1 e^{j\varphi_1} \delta(\tau - \tau_1) + a_2 e^{j\varphi_2} \delta(\tau - \tau_2) \quad (3.7)$$

as drawn here right (in amplitude).



The effect of time dispersion can thus be studied, equivalently, in two domains : either in the delay domain  $\tau$  by modeling the channel by its impulse response  $h(\tau)$ , or in the (baseband) frequency domain, by modeling the channel by  $H(f)$ .

This emphasizes the third wireless channel duality :

#### Channel Duality 3

Baseband frequency  $\Longleftrightarrow$  Delay

## 3.2 Stochastic wideband model

The time-variant transfer function is, from (3.2),

$$H(f, t) = \sum_{n=1}^N a_n e^{j\varphi_n(t)} e^{-j2\pi f \tau_n} \quad (3.8)$$

where, as usual, the amplitude  $a_n$  are assumed constant during the observation time.

If the receiver and/or the IO's are moving, or if the channel is measured at different places of a local area, we know from Chapter 2 that the phases  $\varphi_n(t)$  in (3.8) are random. A stochastic wideband model can thus be deduced :

$$H(f) = \sum_{n=1}^N a_n e^{j\Phi_n} e^{-j2\pi f \tau_n} \quad (3.9)$$

where  $\Phi_n$  is a random phase with uniform distribution between 0 and  $2\pi$ . Each drawing of these phases gives one possible value of  $H(f)$ , i.e. each drawing gives one temporal or spatial realization of  $H(f)$ . Mean values over these realizations (i.e. time or space averages) will be denoted  $\mathcal{E}[\ ]$ .

### 3.2.1 Frequency correlation and delay spread

Let us derive the frequency correlation between  $f$  et  $f + \Delta f$  :

$$\begin{aligned} R(f + \Delta f, f) &= \mathcal{E}[H(f + \Delta f) H^*(f)] \\ &= \int_{-\infty}^{\infty} \int_{-\infty}^{\infty} \mathcal{E}[h(\tau) h^*(\tau')] e^{-j2\pi(f+\Delta f)\tau} e^{j2\pi f \tau'} d\tau d\tau' \end{aligned} \quad (3.10)$$

MPC's arriving at different delays  $\tau$  and  $\tau'$  are usually assumed to be uncorrelated :

$$\mathcal{E}[h(\tau) h^*(\tau')] \equiv P(\tau) \delta(\tau - \tau') \quad (3.11)$$

where  $P(\tau)$  is referred to as the **Power Delay Profile** (PDP). It gives the power density (per-unit  $\tau$ ) incident onto a local area as a function of propagation delay  $\tau$ . Assumption (3.11) is the Uncorrelated Scattering assumption in the delay domain. By (3.10) and (3.11) :

$$R(\Delta f) = \int_{-\infty}^{\infty} P(\tau) e^{-j2\pi\Delta f \tau} d\tau \quad (3.12)$$

Correlation only depends on  $\Delta f$  (not on  $f$ ). Channel is **Wide Sense Stationary** w.r.t. frequency.

The PDP is the inverse Fourier transform of the frequency correlation function :

$$P(\tau) = \int_{-\infty}^{\infty} R(\Delta f) e^{j2\pi\Delta f \tau} d\Delta f \quad (3.13)$$

The PDP is of outmost importance for high data rate communications. It indicates that the signal arrives with some delay spread at the receiver. If different symbols are sent very close to each others, they can overlap at the receiver. We speak about *Inter-Symbol Interference*, ISI.

Cell	$\sigma_\tau$ [ $\mu$ s]	$\Delta f_c$
Indoor	0,03	5 MHz
Urban	3	50 kHz
Countryside	5	30 kHz

Table 3.1 – Typical delay spreads and coherence bandwidths for different cell sizes.

The absolute value of propagation delay is of no importance. By convention, the propagation delay of the first MPC is chosen as the reference  $\tau = 0$ . The PDP is so defined  $\forall \tau \geq 0$ .

The **Delay spread**  $\sigma_\tau$  characterizes the PDP duration :

$$\sigma_\tau = \sqrt{\frac{1}{P} \int_0^\infty \tau^2 P(\tau) d\tau - \tau_m^2} \quad (3.14)$$

where  $P$  is the total power :

$$P = \int_0^\infty P(\tau) d\tau \quad (3.15)$$

and  $\tau_m$  the mean delay :

$$\tau_m = \frac{1}{P} \int_0^\infty \tau P(\tau) d\tau \quad (3.16)$$

Table 3.1 gives typical values for  $\sigma_\tau$ . The larger the communication range, the larger the delay spread since the MPC's follow propagation paths with important length differences.

Experiments show that the PDP can be very often modeled by an exponential :

$$P(\tau) = P_0 e^{-\tau/\sigma_\tau} \quad \tau \geq 0 \quad (3.17)$$

Frequency correlation function can be deduced from (3.12) :

$$R(\Delta f) = \int_{-\infty}^\infty P(\tau) e^{-j2\pi\Delta f \tau} d\tau = \int_0^\infty P_0 e^{-\tau/\sigma_\tau} e^{-j2\pi\Delta f \tau} d\tau = \frac{P_0 \sigma_\tau}{1 + j\sigma_\tau 2\pi \Delta f} \quad (3.18)$$

Those PDP and frequency correlation function are drawn in Figure 3.2.

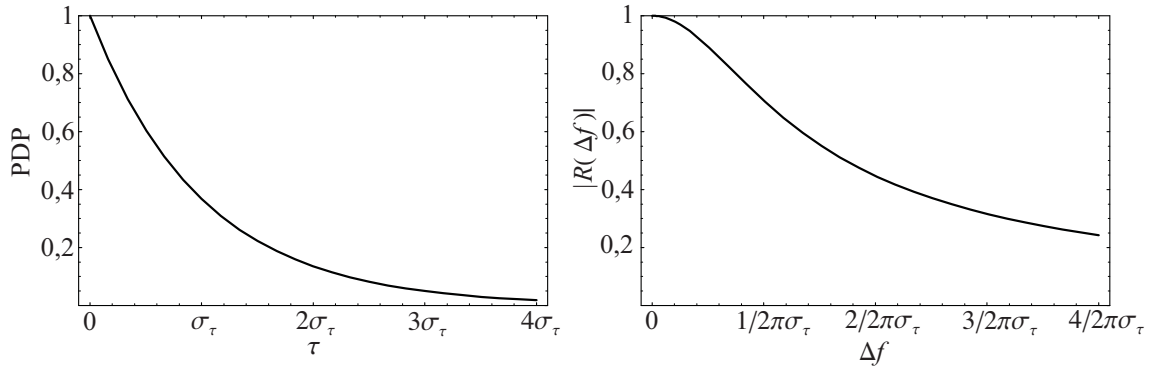


Figure 3.2 – Power Delay Profile et frequency correlation function amplitude in the exponential model (normalized).

### 3.2.2 Coherence bandwidth

The channel **coherence bandwidth**  $\Delta f_c$  is defined as the bandwidth over which correlation is above a given threshold (typically 0.7). As shown in the exponential model,  $\Delta f_c$  is inversely proportional to the delay spread. The precise relation between both parameters depends on the PDP shape, but typically :

$$\Delta f_c \simeq \frac{1}{2\pi \sigma_\tau} \quad (3.19)$$

If the signal bandwidth  $B$  is smaller than  $\Delta f_c$ , all signal frequencies will experience about the same channel gain  $H(f)$ . We are in flat fading. Otherwise, the channel must be modeled taking into account *frequency selective fading*.

This property can be equivalently seen in the delay domain : if the symbol duration  $T_S$  is larger than the channel delay spread  $\sigma_\tau$ , there is no inter-symbol interferences. We are in flat fading. Otherwise, symbols overlap at the receiver : we are in frequency selective fading.

## Frequency characterization

Baseband frequency  $\Longleftrightarrow$  Delay

Channel frequency dependence is due to the differences in propagation delays of the MPC's, i.e. to the channel time dispersion. It can be studied either in the frequency domain via  $H(f)$  or in the delay domain via  $h(\tau)$ , which, in the time-invariant or quasi-static approximations, is

$$h(\tau) = \int_{-\infty}^{\infty} H(f) e^{j2\pi f \tau} df$$

## Frequency correlation

Channel frequency correlation is deduced from the **Power Delay Profile**  $P(\tau)$  :

$$R(\Delta f) = \int_{-\infty}^{\infty} P(\tau) e^{-j2\pi \Delta f \tau} d\tau$$

When the **Delay spread**  $\sigma_\tau$  increases, the channel **Coherence bandwidth**  $\Delta f_c$  decreases. Typically

$$\Delta f_c \simeq \frac{1}{2\pi \sigma_\tau}$$

where  $\sigma_\tau$  is the **delay spread** of the PDP.

If  $B$  is the signal bandwidth :

$$\begin{aligned} \Delta f_c &> B && \text{flat fading} \\ \Delta f_c &< B && \text{frequency selective fading} \end{aligned}$$

Equivalently, if  $T_S$  is the symbol duration :

$$\begin{aligned} \sigma_\tau &< T_S && \text{flat fading} \\ \sigma_\tau &> T_S && \text{frequency selective fading} \end{aligned}$$

In case of flat fading, there is no inter-symbol interference (ISI)

### 3.3 Tapped Delay Line models

We saw in Chapter 1 that the receiver cannot discriminate all MPC's : if  $B$  is the signal bandwidth, all waves arriving during a delay *tap* of duration  $\Delta\tau = 1/2B$  sum up at the receiver. In slow fading, the channel impulse response can be written as a Tapped Delay Line model (1.22) :

$$h_{\text{TDL}}(\tau, t) = \sum_{l=0}^L h_l(t) \delta(\tau - l\Delta\tau) \quad (3.20)$$

where

$$h_l(t) = \sum_{n=1}^N \alpha_n(t) \text{sinc}\left(2B(\tau_n - l\Delta\tau)\right) \quad (3.21)$$

or under the uncorrelated scattering assumption :

$$h_l(t) \simeq \sum_{\tau_n \in \text{tap } l} \alpha_n(t) = \sum_{\tau_n \in \text{tap } l} a_n(t) e^{j\phi_n(t)} e^{-j2\pi f_c \tau_n} \quad (3.22)$$

The channel impulse response is so made of  $L$  taps, where each tap includes several MPC's that the receiver cannot discriminate. The propagation delay of the first tap  $\tau_1$  is conventionally chosen as  $\tau_1 = 0$ .

Since each tap is made of several waves that sum up at the receiver, it experiences fading. **Each tap must so be modeled by a narrowband model** : Rayleigh or Rice fading, random phase with uniform distribution, and specific Doppler spectrum. A typical example of tap spatial fading is drawn in Figure 3.4.

The power delay profile PDP can be computed as

$$P(\tau_n) = \mathcal{E} [ |h_n|^2 ] \quad (3.23)$$

For standardization purposes, wideband models are given in terms of an impulse response model which is typical to the communication scenario : PDP, tap fading (Rayleigh or Rice), Doppler spectrum of each tap.



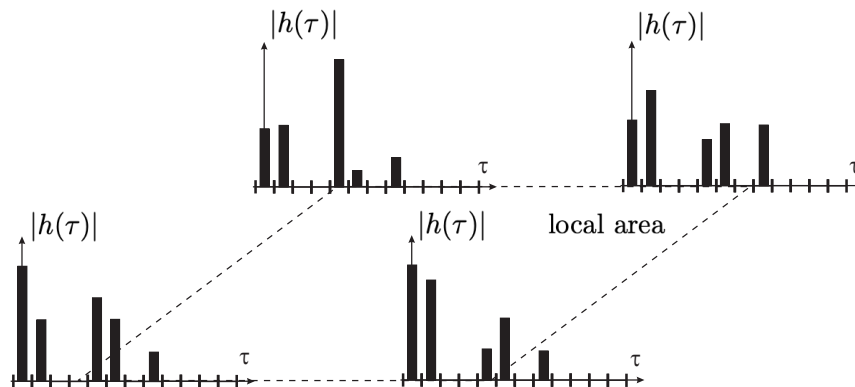


Figure 3.3 – Typical spatial fading of channel impulse response

**Example**

Channel models for 3G communication have been standardized by ITU. For communication to a pedestrian in a urban environment, the channel impulse response includes 6 taps :

Tap	$\tau_n$ [ $\mu$ s]	$P(\tau_n)$ [dB]	Fading	Doppler spectrum
1	0	0	Rayleigh	Clarke
2	0,2	-0,9	Rayleigh	Clarke
3	0,8	-4,9	Rayleigh	Clarke
4	1,2	-8,0	Rayleigh	Clarke
5	2,3	-7,8	Rayleigh	Clarke
6	3,7	-23,9	Rayleigh	Clarke

Experiments show that the MPC's propagate as bundles in the delay and angular domains : the receiver sees different packets of MPC's arriving around the same delay and coming from about the same direction. Those packets are referred to as **clusters**. Clusters are intuitive on physical grounds : each IO has a complex shape that reflects waves with a slight delay and angular dispersion, so producing packets of MPC's. Models that incorporate clusters are referred to as **Cluster Delay Line** models : each incident cluster is characterized by its mean delay, delay spread, mean angle of incidence and angular spread. In each cluster, the MPC's are then modeled by a TDL model.

### 3.4 Example : channel models for 60GHz WLAN systems

Specific channel models are required for 60GHz systems due to the small wavelength compared to classical indoor communication systems. One standardized channel model has been developed in the framework of the IEEE 802.11ad group. We will give here the key ingredients of this model, in the SISO case, and neglecting the polarization aspects.

#### 3.4.1 Principal rays calculation

As we know, 60GHz MPC's suffer from very high losses due to reflection and diffraction. By using ray-tracing, single and double reflected rays are enough in order to provide accurate results w.r.t propagation delays and incidence angle of the MPC's onto the receiver.

So, the first step in generating a 60GHz channel impulse response is to place a transmitter and a receiver in a given indoor environment, and to calculate the LOS, single and double reflected rays by classical ray-tracing approach. A set of realizations can be obtained by moving the transmitter and/or the receiver through the environment. A typical example is shown in Figure 3.4 for a conference room.

Due to people and furniture, some of these rays will, however, be blocked. Channel models include the probability for each ray to be blocked. This probability was derived from ray-tracing simulations and random-walk models for people moving through the environment. This probability is highly dependent on the communication scenario. For instance, a ray reflected off the ceiling has a quasi null probability of being blocked. On the contrary, double reflected rays off the walls are more subject to blockage due to longer propagation paths.

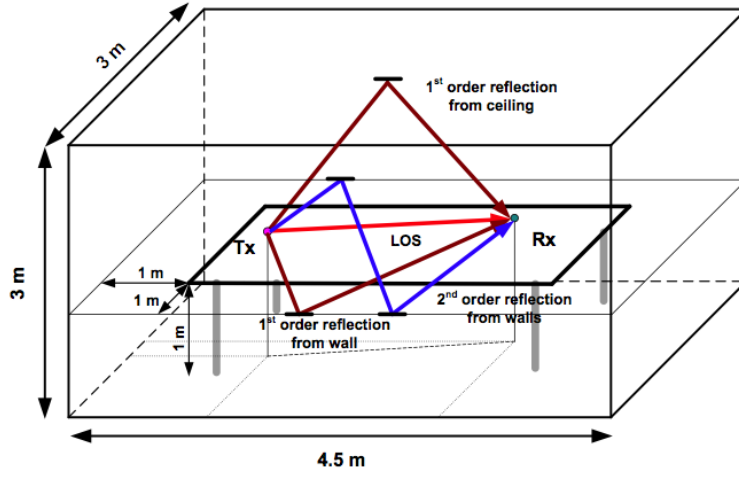


Figure 3.4 – 3D model of a conference room used for ray-tracing. Both TX and RX are located on a table. (A. Maltsev. *et al.*, doc. : IEEE 802.11-09/0334r8, 2010)

#### Example

Let us consider the conference room scenario in Figure 3.4. The probability for the rays to be blocked depends on the chosen communication scenario, LOS or NLOS, that must be fixed a priori. It has been found that :

- Each single reflected ray on the ceiling has a null probability of being blocked
- Single reflected rays off the walls have equal probability to be blocked (0.24) but simultaneous blockage of several rays has a null probability.
- The same holds for double reflected rays off wall and ceiling with blockage probability equal to 0.037.
- Several second order reflected rays off the walls can be blocked simultaneously. The number  $k$  of simultaneously blocked rays is given by a binomial distribution, with the total number of rays  $n = 8$ , and the individual probability of being blocked  $p = 0.175$  :

$$f(k; n; p) = \binom{n}{k} p^k (1 - p)^{n-k} \quad (3.24)$$

### 3.4.2 Intra-clusters parameters

If the IO's, the walls and ceiling were perfect reflectors, with no roughness, no heterogeneity, and if no other small reflectors (small objects) were present in the environment,

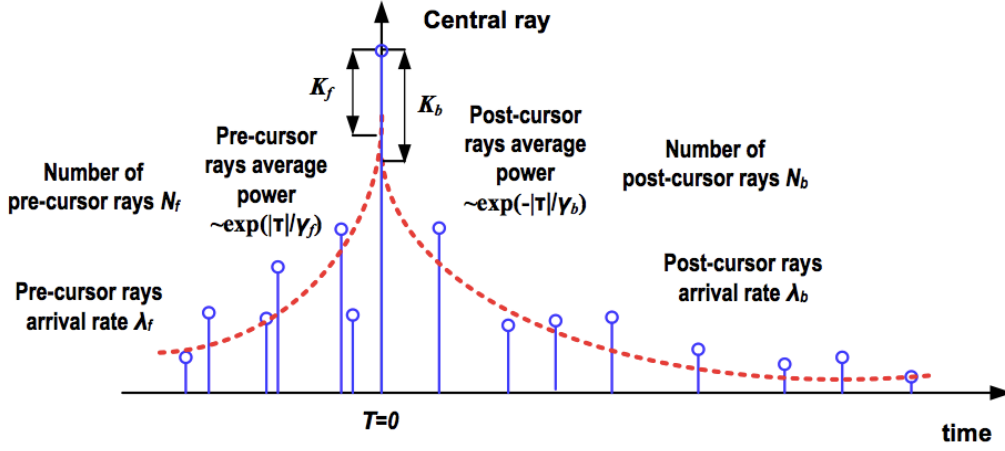


Figure 3.5 – Delay domain model of a cluster (A. Maltsev. *et al.*, doc. : IEEE 8021.11-09/0334r8, 2010)

the rays given by ray-tracing should be the only MPC's propagating from TX to RX. In real-world environments, it is rather found that rays arrive at the receiver as bundles referred to as **clusters**. Each cluster is made of several rays grouped in the delay and the angular domain. The central characteristics of these clusters (arrival time  $\tau_i$  and incidence angle of the central ray) are well predicted by ray-tracing as described here above, but the spread of the rays inside each cluster can only be derived by experiments.

A cluster structure in the delay domain is shown in Figure 3.5. The cluster  $i$  consists of a central ray with fixed amplitude  $\alpha_0^{(i)}$  (given by ray-tracing) and a set of pre-cursors with amplitudes  $\alpha_{-1}^{(i)}.. \alpha_{-N_f}^{(i)}$  and post-cursors  $\alpha_1^{(i)}.. \alpha_{N_b}^{(i)}$ . The number of pre-cursors and post-cursors depends on the scenario.

The arrival time of the central ray is chosen as the reference  $\tau = 0$ . The mean amplitude of the pre-cursors  $A_f^{(i)}(\tau)$  and post-cursors  $A_b^{(i)}(\tau)$  decays exponentially :

$$\begin{aligned} A_f^{(i)}(\tau) &= A_f^{(i)}(0) e^{|\tau|/\gamma_f} \\ A_b^{(i)}(\tau) &= A_b^{(i)}(0) e^{-\tau/\gamma_b} \end{aligned} \quad (3.25)$$

where the decay rates  $\gamma_f$  and  $\gamma_b$  are experimentally found. The peak amplitudes  $A_f^{(i)}(0)$  and  $A_b^{(i)}(0)$  are deduced from the amplitude of the central ray  $\alpha_0^{(i)}$  by two experimental

parameters :

$$\begin{aligned} K_f &= 20 \log \left| \frac{\alpha_0^{(i)}}{A_f^{(i)}(0)} \right| \\ K_b &= 20 \log \left| \frac{\alpha_0^{(i)}}{A_b^{(i)}(0)} \right| \end{aligned} \quad (3.26)$$

The actual values of the pre- and post-cursors amplitudes  $\alpha_k^{(i)}$  obey Rayleigh distributions. Finally, for normalization, the total power of the cluster (sum of the ray powers) is set to one.

The propagation delays  $\tau_k^{(i)}$  around the central ray are deduced from the fact that the pre-cursors and post-cursors are modeled as two Poisson processes with arrival rates  $\lambda_f$  and  $\lambda_b$  (also depending on the scenario).

We finally get the mathematical expression of the normalized impulse response for the cluster  $i$  :

$$\tilde{c}^{(i)}(\tau) = \sum_k \alpha_k^{(i)} \delta(\tau - \tau_k^{(i)}) \quad (3.27)$$

where the propagation delay of the central ray  $\tau_0^{(i)}$  is zero.

In the angular domain, the pre- and post-cursors are spread around the central ray whose incidence angles are deduced from ray-tracing. It is experimentally found that the azimuth and elevation angles of each ray can be drawn from a normal distribution with zero mean and 5 degrees std around the central ray angles.

Table 3.2 summarizes the experimental parameters for the scenario in Figure 3.5.

### 3.4.3 Cluster amplitudes

With the procedure described above, we have now a set of clusters whose total powers are normalized, and whose central propagation delay is zero. The last step in the modeling process is to affect an amplitude to each cluster, and the correct propagation delay .

Parameter	Value
$K_f$	10 dB
$\gamma_f$	3.7 ns
$\lambda_f$	$0.37 \text{ ns}^{-1}$
$N_f$	6
$K_b$	14.2 dB
$\gamma_b$	4.5 ns
$\lambda_b$	$0.31 \text{ ns}^{-1}$
$N_b$	8

Table 3.2 – Clusters parameters for the conference room channel model (A. Maltsev. *et al.*, doc. : IEEE 8021.11-09/0334r8, 2010)

### LOS ray

The first "cluster" is the LOS path, which is modeled by a single ray with amplitude given by the Friis formula with the antenna gains excluded :

$$A_0 = \frac{\lambda}{4\pi d} \quad (3.28)$$

### NLOS clusters

The amplitude of each cluster  $i$  is also deduced from ray-tracing :

$$A_i = g^{(i)} \frac{\lambda}{4\pi d} \quad (3.29)$$

where  $d$  is total propagation distance of cluster  $i$ , and  $g^{(i)}$  a reflection loss given by ray-tracing (typical value around -10dB for single reflected rays and -16dB for double reflected rays).

### 3.4.4 Channel impulse response

We finally get the global (unnormalized) impulse response of the 60GHz channel, by summing the cluster impulse responses shifted in the delay domain :

$$h(\tau) = \sum_i A_i \tilde{c}^{(i)}(\tau - \tau_i) \quad (3.30)$$

where  $\tau_i$  is the propagation delay of the central ray of cluster  $i$  (computed by ray-tracing).